Structure of low-lying states in ^{128}Ba from γ-γ angular correlations and polarization measurements

A. Wolf,[1,2,3] N. V. Zamfir,[1,2] M. A. Caprio,[1] Z. Berant,[1,2,3] D. S. Brenner,[2] N. Pietralla,[1] R. L. Gill,[4] R. F. Casten,[1] C. W. Beausang,[1] R. Kruecken,[1] K. E. Zyromski,[1] C. J. Barton,[1] J. R. Cooper,[1] A. A. Hecht,[1] H. Newmann,[1] J. R. Novak,[1] and J. Cederkall[1,5]

[1]*Wright Nuclear Structure Laboratory, Yale University, New Haven, Connecticut 06520*
[2]*Chemistry Department, Clark University, Worcester, Massachusetts 01610*
[3]*Nuclear Research Center Negev, Beer-Sheva, Israel*
[4]*Brookhaven National Laboratory, Upton, New York 11973*
[5]*CERN, Geneva Switzerland*

(Received 1 February 2002; published 27 August 2002)

A study of the low-lying levels of ^{128}Ba was performed using three clover detectors in a compact arrangement. The levels were populated by beta decay of ^{128}La which was produced by the fusion evaporation reaction ^{116}Sn(^{16}O,$1p3n$). γ-γ angular correlations and polarization measurements were performed. The decay properties of several low-lying states were investigated. Spin assignments were made for two states, and several $E2/M1$ mixing ratios were determined. The results are in good agreement with predictions of the O(6) limit of the interacting boson approximation. One of the states is unambiguously determined to be the hitherto unobserved member of the $\tau=4$ multiplet.

DOI: 10.1103/PhysRevC.66.024323 PACS number(s): 23.20.Lv, 21.10.Re, 21.60.Ev, 27.60.+j

I. INTRODUCTION

The proton-rich even-even Ba isotopes around $A=130$ exhibit features that make them of special interest for nuclear structure studies. One of the more interesting features is the sharp transition from vibrational to deformed structure as the number of neutrons decreases. Many collective bands have been found in even-even Ba isotopes in general and in ^{128}Ba in particular [1]. While the band structure is important to our understanding of the interplay between collective and single-particle degrees of freedom, experimental data on the electromagnetic transitions between the low-lying states are needed in order to test the various collective models and thus better understand the structure of these nuclei. For example, the recently developed Q-phonon scheme [2] provides a very simple and intuitive way of the classification of nuclear states within the various low-lying bands. In the Q-phonon scheme, the low-lying collective states are described in terms of the multiple-Q excitations of the ground state. It was shown [3] that the analytical expressions obtained for the wave vectors provide a good approximation of the wave functions obtained by numerical diagonalization of the interacting boson Hamiltonian, even outside its dynamical symmetry limits. In order to test the Q-phonon selection rules it is necessary to compare $E2$ transition rates between low-lying states. Since many of these transitions can have sizable $M1$ admixtures, experimental data on $E2/M1$ mixing ratios is crucial for using the Q-phonon scheme. Moreover, it was suggested [4] that in this region $M1$ transitions may be enhanced compared to axially symmetric nuclei, due to the admixture of mixed-symmetry states in the low-lying state wave functions.

Most of the data on the low-lying states of Ba isotopes are from in-beam spectroscopy studies (see, for example, Ref. [1]) and from β-decay experiments (Refs. [5–11]). Zolnowski and Sugihara [5] have investigated the levels of ^{128}Ba by β decay of ^{128}La. They used the ^{118}Sn(^{14}N,$4n$) reaction to produce ^{128}La and then a He jet to transport the activity to a counting area. The He-jet technique was also used by Idrissi *et al.* [6] to study the levels of ^{124}Ba from β decay. Kirch *et al.* [7] and Siems *et al.* [8] have used the (^{14}N,xn) reaction on Sn isotopes to produce ^{126,128,130}La and have subsequently studied the β decay of these isotopes to the respective barium isotopes using the chopped beam technique. Asai *et al.* [9] used mass separation of neutron-deficient La isotopes to investigate the systematics of excited 0^+ states in $^{124\text{-}130}$Ba by measuring γ-γ correlations with a five-detector system. They also reported [10] several angular correlation results for ^{126}Ba.

In the present work we report measurements of γ-γ angular correlations, relative intensities for decays of low-lying levels, and polarization measurements in ^{128}Ba from β decay of ^{128}La. The emphasis was on obtaining $E2/M1$ mixing ratios for transitions between low-lying states and on making new spin assignments in order to further our understanding of the low-energy band structure of ^{128}Ba. The experiment was performed at the tandem accelerator of the Wright Nuclear Structure Laboratory at Yale University. We used the Moving Tape Collector device which was recently implemented [12] on one of the beamlines at this laboratory. A 100 MeV ^{16}O beam with an intensity of about 10 pnA was used to produce the parent ^{128}La activity via the reaction ^{116}Sn(^{16}O,$1p3n$)^{128}La. An isotopically enriched, 10 mg/cm^2 target of ^{116}Sn was used. The half-life of ^{128}La is 4.9 min. The activity was deposited onto a 16 mm Kapton tape and transported periodically with a cycle of 10 min for off-beam measurement at the center of an angular correlation setup consisting of three HPGe clover detectors. No significant contribution of any isotope other than ^{128}La was observed. A total of 2.4×10^8 coincidence events were accumu-

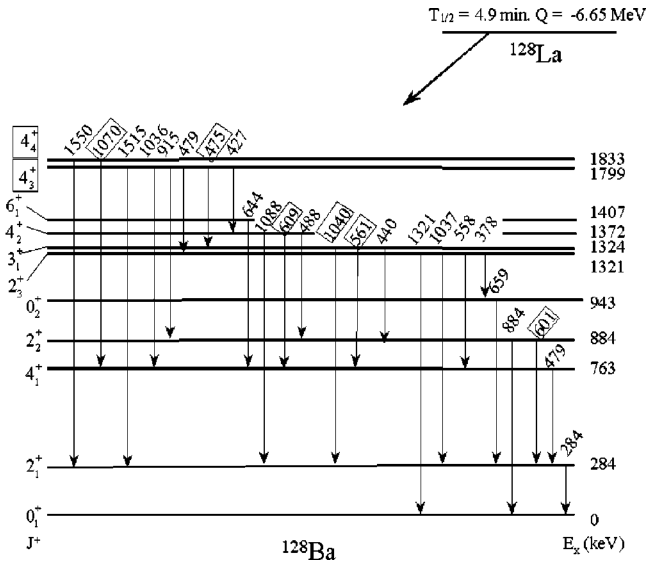

FIG. 1. Partial decay scheme of ^{128}La to ^{128}Ba, showing data relevant to the present work. The two spins in boxes were assigned in this work, and the boxes around energies indicate transitions for which the $E2/M1$ mixing ratios were determined in this work by angular correlations and polarization measurements.

lated in a 5-d run. A partial decay scheme of ^{128}La to ^{128}Ba, showing the transitions relevant to this work is shown in Fig. 1.

II. γ-γ ANGULAR CORRELATIONS

The use of clover detectors for γ-γ angular correlations has the advantage that, when the leaves are considered as separate detectors, a multidetector system in compact geometry is obtained. In addition, the same setup provides polarization data when the clovers are used as Compton polarimeters. The use of the individual leaves of clover detectors for angular correlations and polarization measurements in the same experiment is reported here for the first time. More details of the technique will be presented in a further publication. The three clovers were set around the center of the angular correlation table in two configurations: for the first part of the experiment the three angles between pairs of clovers were 90°, 135°, 135°, and for the second part the angles were 90°, 105°, 165°. The system had 12 leaves, and when only pairs belonging to different clovers were taken into account, a total of 48 pairs were analyzed for γ-γ coincidences. The angles between the individual leaves were calculated using simple geometric relations. The results were sorted in nine groups corresponding to angles between 90° and 180°. In Fig. 2 we present a coincidence spectrum obtained at 93°, with the gate set on the $2_1^+ \rightarrow 0_1^+$, 284 keV transition.

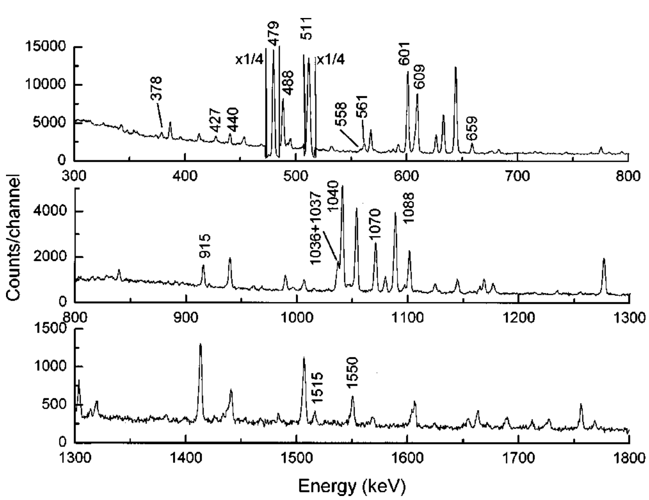

FIG. 2. Coincidence spectrum at 93° for the decay of ^{128}La to ^{128}Ba. The gate was set on the $2_1^+ \rightarrow 0_1^+$, 284 keV transition. The energies of the transitions in Fig. 1 are marked on the respective peaks. Most of the unlabeled peaks also belong to the decay of ^{128}La to ^{128}Ba.

The normalization constants for the correlations were calculated using the strong 479-284 keV, $4_1^+ \rightarrow 2_1^+ \rightarrow 0_1^+$, and 644-479 keV, $6_1^+ \rightarrow 4_1^+ \rightarrow 2_1^+$, cascades in ^{128}Ba. Corrections to the normalization factors due to the different energy dependence of the relative efficiencies of the detectors were

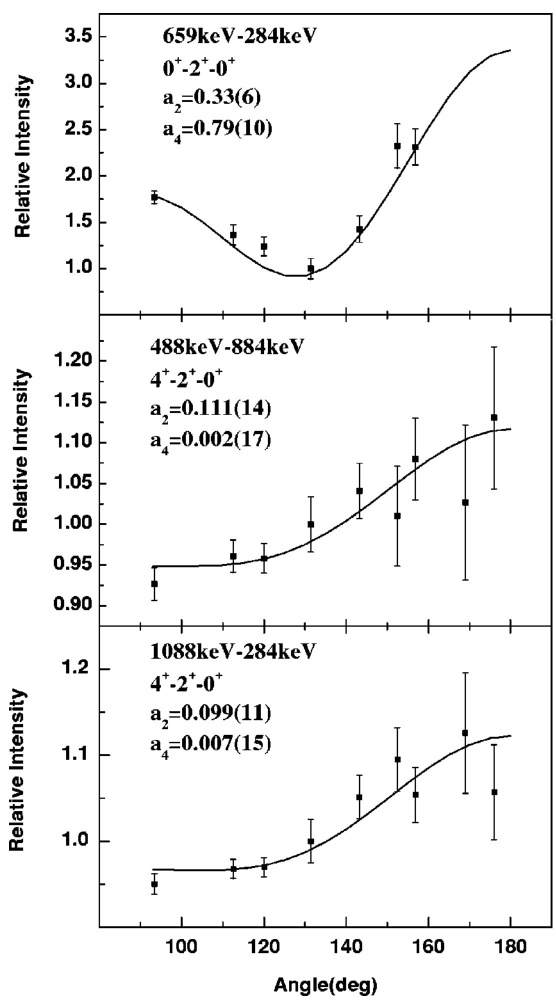

FIG. 3. Angular correlations of the three cascades in ^{128}Ba which were used to test the normalization procedure. The solid lines are fits to a sum of Legendre polynomials. The coefficients a_2, a_4 are not corrected for solid angle attenuation.

TABLE I. The experimental coefficients A_2, A_4 obtained in the present work by fits of the angular correlation data to the sum of Legendre polynomials $1+A_2P_2(\cos\theta)+A_4P_4(\cos\theta)$. The values of A_2, A_4 were corrected for solid angle attenuation.

Cascade (keV)	Spin sequence	A_2	A_4	δ[a]
659-284	$0_2^+\to2_1^+\to0_1^+$	0.36(7)	1.05(13)	$E2$
488-884	$4_2^+\to2_2^+\to0_1^+$	0.120(15)	0.003(22)	$E2$
1088-284	$4_2^+\to2_1^+\to0_1^+$	0.107(12)	0.009(20)	$E2$
601-284	$2_2^+\to2_1^+\to0_1^+$	−0.12(2)	0.29(4)	$+13^{+16}_{-4}$
609-284	$4_2^+\to4_1^+[\to2_1^+]\to0_1^+$	−0.09(3)	0.13(4)	-14^{-16}_{+8}
609-479	$4_2^+\to4_1^+\to2_1^+$	−0.12(2)	0.15(3)	<-20 or >10
561-479	$3_1^+\to4_1^+\to2_1^+$	−0.18(4)	−0.12(5)	$+3.7^{+2.5}_{-1.2}$
1040-284	$3_1^+\to2_1^+\to0_1^+$	−0.032(13)	−0.099(21)	$+4^{+2}_{-1}$
1070-284	$(3,4)\to4_1^+[\to2_1^+]\to0_1^+$	−0.033(22)	0.093(37)	$+0.65^{+0.10}_{-0.10}$ or $-4.0^{+1.0}_{-1.5}$ [b]
475-1040	$(3,4)\to3_1^+\to2_1^+$	0.16(3)	0.10(5)	$+2.0^{+1}_{-0.5}$

[a]Convention of Krane and Steffen [14]; all mixing ratios are for the first transition in the respective cascade.
[b]The polarization data favors the first solution $\delta=+0.65$ (see text).

determined using a ^{152}Eu source. The consistency of the normalization procedure was tested by measuring correlations with pure multipolarities. In Fig. 3 we show the correlations of three such cascades: 659-284 ($0_2^+\to2_1^+\to0_1^+$), 488-884 ($4_2^+\to2_2^+\to0_1^+$), and 1088-284 ($4_2^+\to2_1^+\to0_1^+$). The coefficients a_2, a_4 in Fig. 3 are not corrected for solid angle attenuation. After applying the solid angle correction all the correlation coefficients of these cascades, denoted as A_2, A_4, are in good agreement with the theoretical values (see Table I). The solid angle corrections were calculated using the table of Camp and Van Lehn [13].

In Table I we present the experimental A_2 and A_4 coefficients for all the angular correlations measured in this work. The data of Table I are also shown in Figs. 4, 5, and 6, where the standard ellipses A_4 vs A_2 as a function of the mixing ratio $E2/M1$ are plotted for the relevant spin sequences. The values of the quadrupole to dipole mixing parameter δ in Table I were determined by comparing the experimental correlation coefficients with the theoretical calculations for various values of δ and using the convention of Krane and Steffen [14].

The new results obtained from the angular correlations in this work are the following.

(a) Mixing ratios of the $2_2^+\to2_1^+$, $4_2^+\to4_1^+$, $3_1^+\to2_1^+$, and $3_1^+\to4_1^+$ transitions. All have predominantly $E2$ character.

(b) The spin of the state at 1833 keV, assigned $(3,4^+)$ in Ref. [15], is here unambiguously determined as $J=4$. (See Fig. 2, correlation of the 1070[-479]-284 cascade. The square brackets indicate here and in Table I an intermediate, unobserved transition.)

(c) The spin of the state at 1799 keV, also assigned $(3,4^+)$ in Ref. [15], is also unambiguously determined in the present work as $J=4$. This assignment is obtained from the 475-

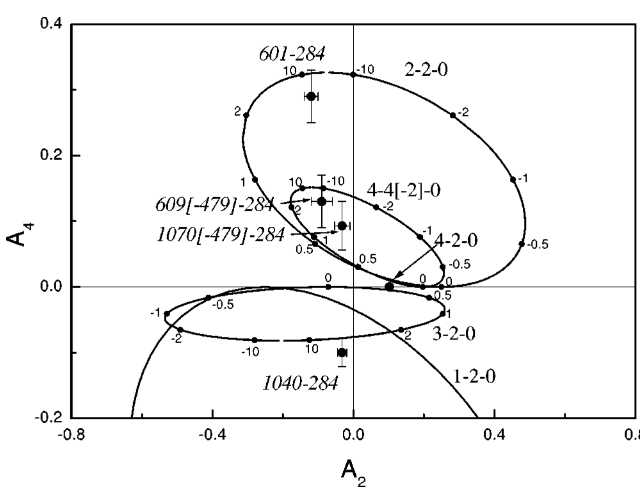

FIG. 4. Angular correlations ellipses A_4 vs A_2 for the range $\delta=-\infty,+\infty$ for the spin sequences J-2-0, $J=1,2,3,4$. The small numbers denote the values of δ for the respective points on the ellipses. The experimental points are results of several γ-γ angular correlations in ^{128}Ba. The square brackets denote unobserved γ transitions. The energies of the γ transitions are in italics.

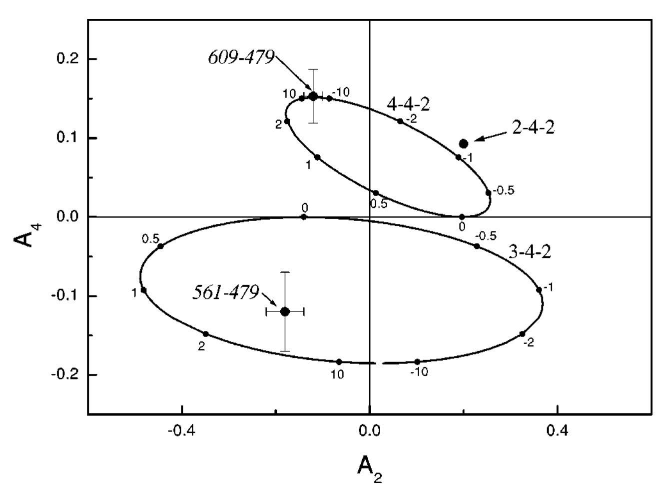

FIG. 5. Angular correlations ellipses A_4 vs A_2 for the range $\delta=-\infty,+\infty$ for the spin sequences J-4-2, $J=2,3,4$. The small numbers denote the values of δ for the respective points on the ellipses. The experimental points are results of two γ-γ angular correlations in ^{128}Ba. The energies of the γ transitions are in italics.

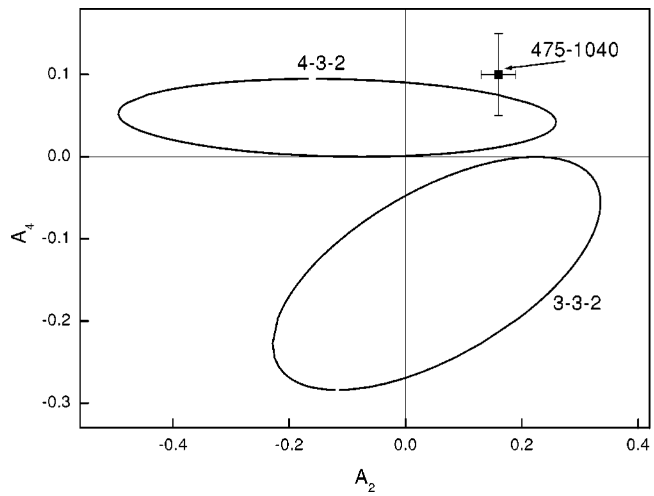

FIG. 6. Angular correlation ellipses for the spin sequences J-3-2, $J=3,4$ for the range $\delta_1=-\infty,+\infty$, where δ_1 is the mixing ratio of the J-3 transition. The mixing ratio for the 3-2 transition was taken as $\delta_2=+4$, as determined from the 1040–284 keV, 3-2-0 correlation (Table I). The experimental point is the result of the correlation measurement for the 475–1040 keV cascade.

1040 keV correlation and using the mixing ratio $\delta(E2/M1)=4^{+2}_{-1}$ for the 1040 keV, $3^+_1\rightarrow 2^+_1$ transition, as determined from the 1040-284 correlation (Fig. 6).

From Fig. 4 we see that while the spin of the state at 1833 keV is unambiguously determined from the 1070[-479]-284 correlation, the mixing ratio of the 1070 keV transition from this state to the 4^+_1 state cannot be extracted from the A_2, A_4 coefficients. The two possible solutions for δ are given in Table I. The polarization measurement will be used to determine the correct value.

III. POLARIZATION MEASUREMENTS

An important advantage of using clover detectors is that they can serve as Compton polarimeters, so polarization data can be obtained in addition to angular correlation data in the same experiment. In our setup two clovers were at 90° with respect to each other, which is the optimum angle for polarization measurements. Appropriate analysis of the data showed that the statistics were good enough to determine the linear polarizations of some of the strong lines in the spectrum. We define here the degree of linear polarization $P_\gamma(\theta)$ as

$$P_\gamma(\theta)=\frac{W(\theta,\phi=0)-W(\theta,\phi=\pi/2)}{W(\theta,\phi=0)+W(\theta,\phi=\pi/2)},$$

where $W(\theta,\phi=0),W(\theta,\phi=\pi/2)$ are the intensities of the γ radiation polarized parallel ($\phi=0$) and perpendicular ($\phi=\pi/2$) to the plane of the γ-γ correlation. θ is the angle between the directions of the two γ rays in the γ-γ correlation. $P_\gamma(\theta)$ depends on the spins and parities of the γ-γ cascade and on the mixing ratios of the transitions involved (see, for example, Ref. [16]). For any given set of parameters $P_\gamma(\theta)$ has its maximum at $\theta=90°$. The experimentally measured quantity is the asymmetry ratio $A_\gamma(\theta)$, which is defined as

$$A_\gamma(\theta)=\frac{aN_\perp-N_\parallel}{aN_\perp+N_\parallel},$$

where $N_\perp,N_\parallel$ are the number of Compton-scattered photons from the central detector perpendicular and parallel to the correlation plane. The parameter a takes into account the instrumental asymmetry of the polarimeter and has to be determined experimentally. In an ideal apparatus a should be equal to 1 for all γ ray energies. The relation between A_γ and P_γ is given by the equation

$$A_\gamma(\theta)=Q(E_\gamma)P_\gamma(\theta),$$

where $Q(E_\gamma)$ is the polarization sensitivity of the system and has to be known in order to extract the linear polarization $P_\gamma(\theta)$ from the measured A_γ. The sensitivity of the clovers used in our experiment was determined using an ^{152}Eu source. In Fig. 7 we show the measured Q as a function of energy. Also shown in this figure are the results of the Monte Carlo calculations of $Q(E_\gamma)$ of Garcia-Raffi *et al.* [17]. We see that the agreement with the calculation is quite good, so we can confidently combine the experimental and calculated values in order to obtain the polarization efficiencies for the ^{128}Ba data. The instrumental asymmetry a was measured by gating on the 511 keV line. All the γ-rays in coincidence with this line should be unpolarized and therefore can be used to check the instrumental asymmetry of the setup. In Fig. 8 we present the measured values of a as a function of energy. We see that the asymmetry parameter a is one within the error bars, except for the 284 keV line, where a slight nonzero asymmetry was observed. This effect was taken into account in the data analysis.

Our setup and data acquisition system enable the determination of the linear polarization of both components of any

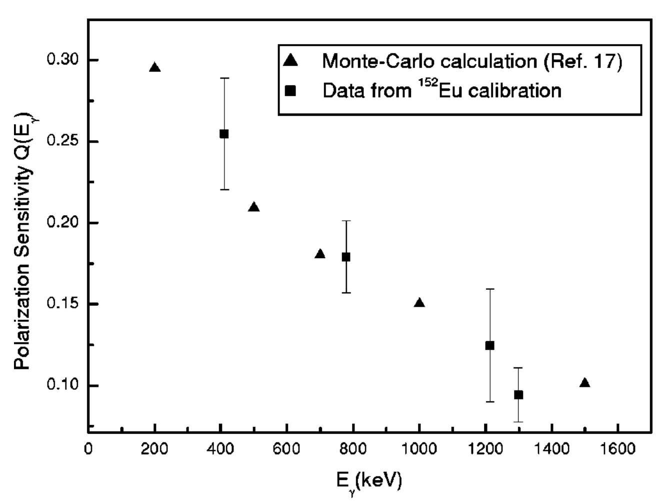

FIG. 7. The polarization efficiency Q vs γ energy E_γ for the clover detector used in this experiment (see text). The experimental points are from the calibration with the ^{152}Eu source. The triangles are Monte Carlo calculations of Garcia-Raffi *et al.* [17].

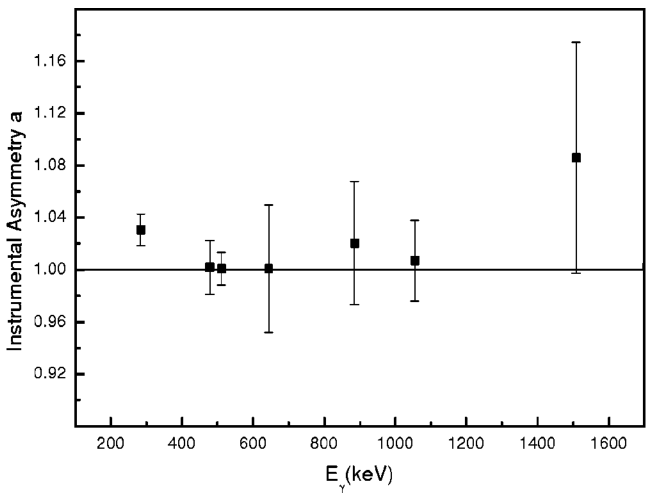

FIG. 8. The instrumental asymmetry a of the clover detector polarimeter. The results are from cascades in which one of the transitions is the 511 keV line (see text).

γ-γ cascade, provided the statistics are good enough. Therefore, for any given correlation we can, in principle, determine two parameters P_γ (first transition) and P_γ (second transition), both of which depend on the spins, parities, and mixing ratios of the γ-γ cascade and can thus resolve ambiguities that were not resolved by the γ-γ correlation. As an example, we show in Fig. 9 the experimental values of P (first) and P (second) for the 609-479 keV cascade. The ellipse in this figure was calculated for a $4^+ \rightarrow 4^+ \rightarrow 2^+$ cascade as a function of the mixing ratio of the first transition. We see that the polarization result is consistent with the mixing ratio determined by the angular correlation (Table I).

In Fig. 10 we show the polarization results for the 1070-479 cascade. In this case, the angular correlation could not determine the mixing ratio unambiguously and two solutions were obtained (Table I). From Fig. 10 we see that the polarization slightly favors the solution $\delta_1(E2/M1) = +0.65(10)$ for the 1070 keV transition. Finally, in Fig. 11 we present the polarization results for the 659-284 $(0 \rightarrow 2^+ \rightarrow 0^+)$ cascade. The state at 943 keV decaying by the 659 keV transition was determined to have $J=0$ by Asai *et al.* [9] From Fig. 11 we conclude that the character of the first transition is $E2$ and the parity of this $J=0$ state is positive.

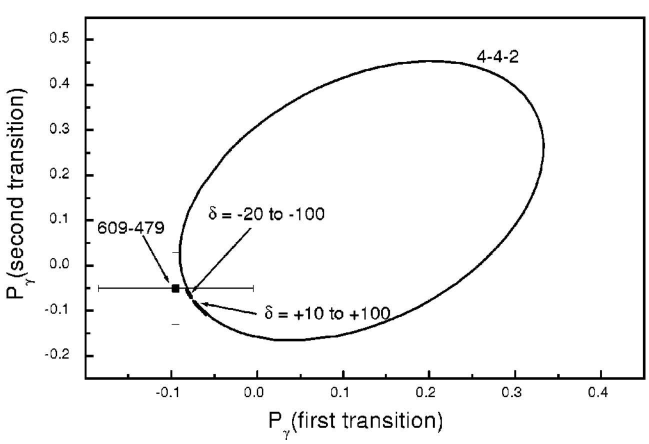

FIG. 9. Polarization results for the 609–479 keV cascade and plot of the polarization of the second transition vs the polarization of the first transition for a 4-4-2 cascade for the range $\delta = -\infty, +\infty$. δ is the mixing ratio of the first transition. The ellipse was calculated assuming no change of parity for the first transition, and that the second transition is $E2$. The range of the mixing ratio δ from the angular correlation measurement of the same cascade (Table I) is shown on the ellipse. The measured polarizations agree with $>99\%$ $E2$ character of the $4_2^+ \rightarrow 4_1^+$ transition.

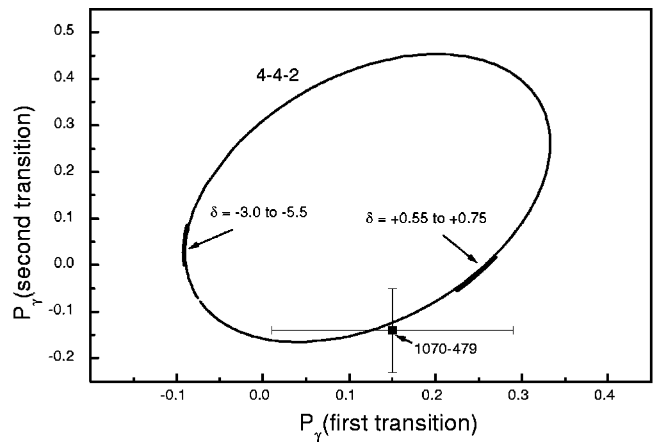

FIG. 10. Polarization results for the 1070–479 keV cascade and plot of the polarization of the second transition vs the polarization of the first transition for a 4-4-2 cascade for the range $\delta = -\infty, +\infty$. δ is the mixing ratio of the first transition. The ellipse was calculated assuming no change of parity for the first transition and that the second transition is $E2$. The two ranges of the mixing ratio δ from the angular correlation measurement of the same cascade (Table I) are shown on the ellipse.

IV. DECAY PROPERTIES OF LOW-LYING STATES

In the present work we determined that the states at 1799 and 1833 keV both have $J=4$. In order to identify their structure within a nuclear model we need to know the decay

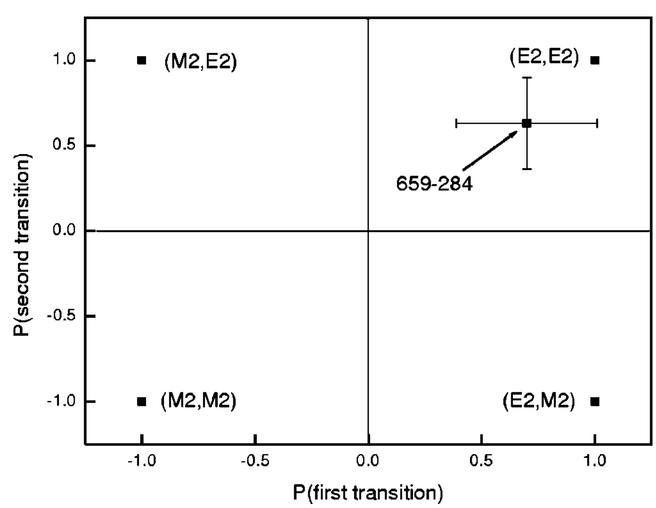

FIG. 11. Polarization result for the 659–284 keV, $0_2^+ \rightarrow 2_1^+ \rightarrow 0_1^+$, cascade and the calculated values for the four possible combinations of polarities of the transitions.

TABLE II. Relative intensities and relative $B(E2)$ values for transitions of states in ^{128}Ba to lower-lying levels, compared with an IBA calculation (see text).

Level energy (keV)	E_γ (keV)	J_i^π	J_f^π	Relative intensity	Experimental relative $B(E2)$[a]	Calculated $B(E2)$ (W.u.)[b]
884	601	2_2^+	2_1^+	100	103	103
	884	2_2^+	0_1^+	84(10)	12(1)	0-11[c]
1321	378	2_3^+	0_2^+	32(5)	40	40
	436	2_3^+	2_2^+	<12	<7	0-10[c]
	558	2_3^+	4_1^+	7(2)	1.2(4)	0-3[c]
	1037	2_3^+	2_1^+	100	0.8(2)	0-0[c]
	1321	2_3^+	0_1^+	31(6)	0.10(2)	0-0[c]
1324	440	3_1^+	2_2^+	21(2)	79	79
	561	3_1^+	4_1^+	12(1)	13(2)	32
	1040	3_1^+	2_1^+	100	5(1)	0-11[c]
1372	488	4_2^+	2_2^+	98(13)	58	58
	609	4_2^+	4_1^+	82(10)	16(3)	53
	1088	4_2^+	2_1^+	100	1.1(2)	0-8[c]
1799	392	4_3^+	6_1^+	<2	<8	1
	427	4_3^+	4_2^+	24(2)	63(10)	50
	475	4_3^+	3_1^+	37(5)	57	57
	479	4_3^+	2_3^+	8(3)	12(5)	0-1[c]
	915	4_3^+	2_2^+	100	6(1)	0-9[c]
	1036	4_3^+	4_1^+	37(5)	1.2(2)	0-1[c]
	1515	4_3^+	2_1^+	28(8)	0.13(4)	0-0[c]
1833	461	4_4^+	4_2^+	<2	<10	0-4[c]
	949	4_4^+	2_2^+	<1	<0.14	0-0[c]
	1070	4_4^+	4_1^+	100	2.2(4)	0-0[c]
	1550	4_4^+	2_1^+	35(5)	0.40(6)	0-0[c]
	509	4_4^+	3_1^+	<9	<27	0-4[c]
	513	4_4^+	2_3^+	<17	<49	49
1710	389	0_3^+	2_3^+	<5	<33	0-0[c]
	825	0_3^+	2_2^+	<9	<1	0-13[c]
	1426	0_3^+	2_1^+	100	1	0-0[c]
2219	898	0_4^+	2_3^+	<10	<5	0-1.5[c]
	1334	0_4^+	2_2^+	<21	<1.5	0-0[c]
	1935	0_4^+	2_1^+	100	1	0-0.2[c]

[a]The relative $B(E2)$ obtained from the relative intensities in this work were normalized for each initial state to the value of the largest calculated $B(E2)$ for that state given in column 7, except for the 0_3^+,0_4^+ states for which the upper limits for the $B(E2)$ were normalized to a value of 1 for the observed transitions to the 2_1^+ state.

[b]The effective charge for the calculation was taken from the experimental value $B(E2;2_1^+\rightarrow 0_1^+)=76$ W.u. [1], $e_2=0.12$ eb $=2$ W.u.$^{1/2}$.

[c]The two values were calculated with $\chi=0$ and $\chi=-\sqrt{7}/2$, respectively, in the $T(E2)$ operator.

properties of all low-lying states. Part of the required information exists in the literature [15]. However, the states at 943 keV (0_2^+) and 1321 keV (2_3^+) do not appear in Ref. [15]. Therefore, it was important to determine the decay properties of all the low-lying levels using the data from the present experiment. To this purpose the data from all detectors were sorted into one γ-γ coincidence matrix. The relative efficiency of the system as a function of energy was determined from the coincidence matrix using the known part of the decay scheme. Relative intensities were obtained by placing energy gates on various transitions leading into and from the relevant low-lying excited states and using the relative efficiency calibration. We extracted the relative intensities of the transitions from all the states up to 1833 keV with spin less or equal to 4. Special care was taken to subtract contributions of lines whose energies were close to those of the lines of interest, and in several cases the relative intensities were determined in several ways in order to check the consistency of the results. We also included upper limits for the decay of the 0_3^+ and 0_4^+ states which were determined by Asai *et al.* [9] to be at 1710 and 2219 keV, respectively. In Table II we present the relative intensities and relative $B(E2)$ values for the decays of the low-lying levels, as determined in this work. Since the 0_2^+ state experimentally decays only to the 2_1^+ state, we did not include it in the table.

V. DISCUSSION AND CONCLUSIONS

The neutron-deficient Ba isotopes exhibit collective properties which are considered to be well described by the O(6) symmetry of the interacting boson approximation (IBA) [18,19]. We therefore attempt to interpret the new as well as the existing data for ^{128}Ba in the framework of the O(6) limit. The Hamiltonian in this case is

$$H=-kQ^{\chi=0}\cdot Q^{\chi=0},$$

where $Q^{\chi=0}\equiv Q(\chi=0)$ is a particular form [generator of O(6)] of the general IBA quadrupole operator $Q=(s^\dagger d+sd^\dagger)+\chi(d^\dagger d)^2$. The parameter χ varies in the IBA between 0 and $-\sqrt{7}/2$. The $E2$ operator is

$$T(E2)=e_2 Q,$$

where e_2 is the boson effective charge. In the last column of Table II we present the calculated transition probabilities for $\chi=0$ in the $T(E2)$ operator which corresponds to the O(6) limit in the consistent Q formalism [20]. In Fig. 12 we present a comparison of the low-lying experimental levels and a calculation using the above Hamiltonian. We see that the agreement is quite good.

A nonzero χ value in the $T(E2)$ operator was introduced in Ref. [21] to reproduce the weak transitions which are forbidden in the O(6) symmetry. The allowed transitions in O(6) [with $\Delta\tau=\pm 1$, where τ is the quantum number of the O(5) group [22]] are not affected by the parameter χ of the $T(E2)$ operator. For transitions which are forbidden in pure O(6) (i.e., $\Delta\tau=0,\pm 2$ transitions) we also calculated the $B(E2)$ values using the largest possible value of the χ parameter, $\chi=-\sqrt{7}/2$, and therefore for these transitions we have two calculated values in Table II: one is zero [pure O(6)] and the other is usually finite and corresponds to the maximum absolute value of χ. The calculated values in Table II are all given in Weisskopf units (W.u.) and were calculated with

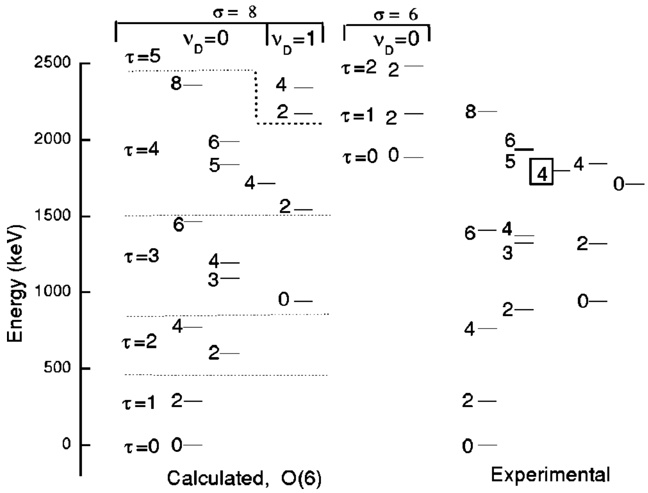

FIG. 12. Positive parity levels of ^{128}Ba calculated for the O(6) limit of the IBA. σ, τ, and ν_Δ are the O(6), O(5), and additional quantum number, respectively. The dotted lines separate states within a given τ multiplet. Also shown are the low-lying experimental levels. The level within the box is the hitherto unobserved $J=4$ member of the $\tau=4$ multiplet (see text).

$e_2=0.12$ eb obtained from normalizing the $B(E2;2_1^+\to0_1^+)$ value to the experimental value of 76 W.u. [1]. For comparison purposes, for each initial state we normalized the experimentally determined relative $B(E2)$ values to the largest calculated $B(E2)$ value from that state. From Table II we see that, except for the 4_4^+ state, all relative B(E2) values are consistent with the calculation. In particular, the data for the decay of the 4_3^+ state, whose spin was determined in the present work, show clearly that it decays mostly to the 3_1^+ and 4_2^+ states. This state is therefore the hitherto unobserved 4^+ member of the $\tau=4$ multiplet in the O(6) description of ^{128}Ba [18]. The present data for the decay of the 0_2^+, 0_3^+, 0_4^+, 2_3^+, and 4_4^+ states do not allow a definite interpretation for the structure of these states (Table II and Fig. 12). The 0_2^+, 2_3^+ states are very likely the lowest part of the $\sigma=8$, $\nu_\Delta=1$ sequence, but the very low transition energies (practically zero) to the members of the next lower τ multiplets with $\nu_\Delta=0$, prohibit the detection of the characteristic $\Delta\tau=1$ transitions. The 4_4^+ state is probably part of the same $\nu_\Delta=1$ sequence, but the exact, even large, relative strength of the 513 keV, $4_4^+\to2_3^+$ transition is difficult to measure. The 0_3^+ and 0_4^+ states are candidates for the $0_{\sigma=6}^+$ state but more data, in particular absolute $E2$ and $E0$ strengths, are necessary to make a final conclusion. On the other hand, the structure of all these states could be affected by quasiparticle configurations, thus placing them outside the framework of the IBA.

In conclusion, in this work we used a setup of three clover detectors and the Moving Tape Collector facility at Yale University to measure properties of low-lying levels of ^{128}Ba following β decay of ^{128}La. The individual leaves of the clover detectors were used as a multidetector apparatus to measure γ-γ angular correlations and polarizations in the same experimental run. We determined the spins of the 1799 and 1833 keV levels in ^{128}Ba, as $J=4$ as well as several mixing ratios and relative $B(E2)$ values for transitions between low-lying levels in this nucleus. The results, when analyzed together with existing data, are in good agreement with the O(6) description for this isotope.

ACKNOWLEDGMENTS

This work was supported by the U.S. DOE under Grant Nos. DE-FG02-91ER-40609, DE-FG02-88ER-40417, and DE-AC02-98-CH10886 and by the DFG under Grant No. Pi393/1-1.

[1] P. Petkov *et al.*, Nucl. Phys. **A640**, 293 (1998); K. Schiffer *et al.*, *ibid.* **A458**, 337 (1986).
[2] T. Otsuka and K.H. Kim, Phys. Rev. C **50**, R1768 (1994); G. Siems *et al.*, Phys. Lett. B **320**, 1 (1994).
[3] N. Pietralla *et al.*, Phys. Rev. Lett. **73**, 2962 (1994); N. Pietralla *et al.*, Phys. Rev. C **57**, 150 (1998).
[4] T. Otsuka, Hyperfine Interact. **75**, 23 (1992).
[5] D.R. Zolnowski and T.T. Sugihara, Phys. Rev. C **16**, 408 (1977).
[6] N. Idrissi *et al.*, Z. Phys. A **341**, 427 (1992).
[7] K. Kirch *et al.*, Nucl. Phys. **A587**, 211 (1995).
[8] G. Siems *et al.*, Proceedings of the 6th International Conference on Nuclei far from Stability and 9th International Conference on Atomic Masses and Fundamental Constants, Bernkastel-Kues, Germany, 1992, p. 675.
[9] M. Asai *et al.*, Phys. Rev. C **56**, 3045 (1997).
[10] M. Asai *et al.*, Nucl. Instrum. Methods Phys. Res. A **398**, 265 (1997).
[11] T. Hayakawa *et al.*, Z. Phys. A **358**, 15 (1997).
[12] N.V. Zamfir and R.F. Casten, J. Res. Natl. Inst. Stand. Technol. **105**, 147 (2000).
[13] D.C. Camp and A.L. Van Lehn, Nucl. Instrum. Methods **76**, 192 (1969).
[14] K.S. Krane and R.M. Steffen, Phys. Rev. C **2**, 724 (1970).
[15] K. Kitao, M. Kanbe, and Z. Matumoto, Nucl. Data Sheets **38**, 191 (1983); www.nndc.bnl.gov
[16] A.J. Ferguson, in *Angular Correlation Methods in Gamma-Ray Spectroscopy* (North-Holland, Amsterdam, 1965), p. 96.
[17] L.M. Garcia-Raffi *et al.*, Nucl. Instrum. Methods Phys. Res. A **391**, 461 (1997).
[18] R.F. Casten and P. von Brentano, Phys. Lett. **152B**, 22 (1985).
[19] P. von Brentano *et al.*, in *Proceedings of the International Symposium on the Frontiers of Nuclear Structure Physics*, Tolyo, Japan, 1994, edited by M. Ishihara, T. Otsuka, T. Mizusaki, and K. Yazaki (World Scientific, Singapore, 1994), p. 82.
[20] R.F. Casten and D.D. Warner, Rev. Mod. Phys. **60**, 389 (1988).
[21] P. Van Isacker, Nucl. Phys. **A465**, 497 (1987).
[22] A. Arima and F. Iachello, Phys. Rev. Lett. **40**, 385 (1978)